Cancer Research

Super-Enhancer–Associated Long Noncoding RNA HCCL5 Is Activated by ZEB1 and Promotes the Malignancy of Hepatocellular Carcinoma

Li Peng[1,2,3], Binyuan Jiang[1,4], Xiaoqing Yuan[2,5], Yuntan Qiu[2,3], Jiangyun Peng[2,3], Yongsheng Huang[2,3], Chaoyang Zhang[1], Yin Zhang[2,3], Zhaoyu Lin[2,6], Jinsong Li[2,6], Weicheng Yao[2,3], Weixi Deng[2,3], Yaqin Zhang[1], Meng Meng[2,3], Xi Pan[7], Chunquan Li[8], Dong Yin[2,3], Xinyu Bi[9], Guancheng Li[1,10], and De-Chen Lin[2,3]

Abstract

Hepatocellular carcinoma (HCC) is one of the most dominant causes of neoplasm-related deaths worldwide. In this study, we identify and characterize *HCCL5*, a novel cytoplasmic long noncoding RNA (lncRNA), as a crucial oncogene in HCC. HCCL5 promoted cell growth, G_1–S transition, invasion, and metastasis while inhibiting apoptosis of HCC cells both *in vitro* and *in vivo*. Moreover, HCCL5 was upregulated in TGF-β1-induced classical epithelial-to-mesenchymal transition (EMT) models, and this lncRNA in turn accelerated the EMT phenotype by upregulating the expression of transcription factors Snail, Slug, ZEB1, and Twist1. HCCL5 was transcriptionally driven by ZEB1 via a super-enhancer and was significantly and frequently overexpressed in human HCC tissues, correlating with worse overall survival of patients with HCC. Together, this study characterizes HCCL5 as a super-enhancer–driven lncRNA promoting HCC cell viability, migration, and EMT. Our data also suggest that HCCL5 may serve as a novel prognostic biomarker and therapeutic target in HCC.

Significance: These findings identify the lncRNA HCCL5 as a super-enhancer–driven oncogenic factor that promotes the malignancy of hepatocellular carcinoma.

Introduction

With approximately 782,000 new cases worldwide in 2012, hepatocellular carcinoma (HCC) is the sixth most common malignancy, and ranks the third most common cause of cancer-related death (1, 2). In the United States, 42,220 new cases and 30,200 deaths were estimated to be from liver cancer in 2018 (3). Alarmingly, in contrast to many other common cancers, the incidence of HCC continues to increase rapidly in women while it seems to reach a peak in men since 2010 (3). In general, HCC has a poor prognosis, with a 5-year survival rate lower than 30% (4, 5), in part, due to lack of effective methods for early detection. Similar to most other cancer types, the survival probability of patients with HCC reduces markedly with increased clinical stages (6, 7). For example, in a large-scale clinical study of 8,510 samples, the 5-year survival rate of HCC patients with stage I, II, III, and IV was 47%, 32%, 20%, and 10%, respectively (8). In addition, our recent work highlighted intratumor heterogeneity at both DNA mutation and methylation levels as a key factor contributing to treatment failure in HCC (9). Therefore, an urgent need exists to better understand the pathogenesis of HCC for the development of biomarkers as well as effective therapeutic regimens.

Long noncoding RNAs (lncRNA) are transcripts over 200 nucleotides that are generally lack of protein-coding potential (10). LncRNAs are involved in many key biological processes, and their dysregulation leads to disease states, including malignancy (11–14). Mechanistically, lncRNAs exert their actions mainly via interaction with RNAs/proteins in the regulation of gene transcription, signaling pathway, and mRNA stabilization (15). Recently, few lncRNAs were reported to be capable of encoding for small peptide (16, 17). However, due to their low expression and lack of developmental conservation in general, the vast majority of lncRNAs are functionally uncharacterized (18).

Superenhancers are described as clusters of stretched enhancers with exceptionally high degree of enrichment for the binding of

[1]Key Laboratory of Carcinogenesis of the Chinese Ministry of Health and the Key Laboratory of Carcinogenesis and Cancer Invasion of Chinese Ministry of Education, Xiangya Hospital, Central South University, Changsha, China. [2]Guangdong Provincial Key Laboratory of Malignant Tumor Epigenetics and Gene Regulation, Sun Yat-Sen Memorial Hospital, Sun Yat-Sen University, Guangzhou, China. [3]Medical Research Center, Sun Yat-Sen Memorial Hospital, Sun Yat-Sen University, Guangzhou, China. [4]Medical Research Center, Changsha Central Hospital, Changsha, China. [5]Breast Tumor Center, Sun Yat-Sen Memorial Hospital, Sun Yat-Sen University, Guangzhou, China. [6]Department of Oral & Maxillofacial Surgery, Sun Yat-sen Memorial Hospital, Sun Yat-sen University, Guangzhou, China. [7]Department of Oncology, the Third Xiangya Hospital, Central South University, Changsha, China. [8]School of Medical Informatics, Daqing Campus, Harbin Medical University, Daqing, China. [9]Department of Hepato-Biliary Surgery, National Cancer Center/Cancer Hospital, Chinese Academy of Medical Sciences and Peking Union Medical College, Beijing, China. [10]Cancer Research Institute, Central South University, Changsha, China.

Note: Supplementary data for this article are available at Cancer Research Online (http://cancerres.aacrjournals.org/).

Corresponding Authors: Guancheng Li, Xiangya Hospital, Central South University, Changsha 410078, China. Phone: 8673-1848-05445; Fax: 8673-1823-55042; E-mail: ligc61@csu.edu.cn; and De-Chen Lin, Sun Yat-Sen Memorial Hospital, Sun Yat-Sen University, Guangzhou 510120, China. Phone: 86-20-89205573; Fax: 86-20-81332601; E-mail: lindch5@mail.sysu.edu.cn

doi: 10.1158/0008-5472.CAN-18-0367

transcriptional factors and coactivators (19). Importantly, super-enhancers are capable of driving much higher levels of transcription and exhibit much stronger lineage and tissue specificity compared with typical enhancers (20). Superenhancers are enriched in genes that play prominent roles in regulating cell identify and differentiation (21–23). Importantly, we recently found that superenhancers are also capable of driving the expression of lncRNAs with tumor-promoting functions (24, 25). It will be of great interest and value to identify and characterize such superenhancer-associated oncogenic lncRNAs in the pathogenesis of HCC.

Epithelial-to-mesenchymal transition (EMT) is a cellular process during which cell-to-cell contacts are lost while obtaining elevated invasiveness to spread to neighboring and distant tissues (26). EMT is essential for embryonic development and has been associated with various diseases. In neural crest cells, EMT-related transcription factors (for example, Snail, Twist, and ZEB1) could promote EMT *in vitro* and *in vivo* (27, 28). In HCC, EMT is considered as an indispensable process that promotes both intra- and extrahepatic metastasis (29, 30). However, whether and how EMT is regulated by lncRNAs remain to be elucidated. This study was aimed at characterizing novel oncogenic lncRNAs in HCC, which might provide new clues facilitating the identification of therapeutic targets as well as biomarkers for diagnosis and prognosis.

Materials and Methods

Screening for noncoding ESTs differentially expressed in HCC

The cDNA xProfiler tool in the Cancer Genome Anatomy Project (CGAP) database (http://cgap.nci.nih.gov/) was applied to screen for noncoding ESTs uniquely expressed in liver cancer samples, through comparing EST libraries between liver cancer samples with pan-cancer samples from other tumor types. As a result, 1,142 candidate ESTs expressed uniquely in liver cancer were identified. Coding transcripts and repeated sequences were filtered out by NCBI BLAST (http://blast.ncbi.nlm.nih.gov/Blast.cgi) with the combination of the NCBI UniGene and EST databases.

Protein-coding potential predictions

The protein-coding potential of transcripts was evaluated using the Coding Potential Calculator (CPC; http://cpc.cbi.pku.edu.cn/), Open Reading Frame (ORF) Finder (http://www.ncbi.nlm.nih.gov/gorf/orfig.cgi), and Pfam 28.0 (http://pfam.xfam.org/) with default parameters. The Conserved Domain Database (CDD; http://www.ncbi.nlm.nih.gov/Structure/cdd/wrpsb.cgi) was applied to predict structural conservation and stable RNA secondary structures in thermodynamics.

Cell culture

Human HCC cell lines HepG2, SMMC-7721 and HCCLM3 were purchased from Xiangya Central Experiment Laboratory of Central South University (Changsha, P.R. China), and detected for *Mycoplasma* before use. Cells were maintained in DMEM or RPMI1640 medium (HyClone) supplemented with 10% heat-inactivated FBS (Gibco), at 37°C in an incubator containing 5% CO_2. G418 (Sigma-Aldrich) and puromycin (Sigma-Aldrich) were used to select for overexpression and shRNA-stable cells, respectively. Cells were treated with 10 ng/mL of recombinant TGF-β1 (R&D Systems) for the indicated time with TGF-β1 replenishment every 2 days. The identity of all cell lines was recently verified by short tandem repeat analysis in 2017.

5′ and 3′ rapid amplification of cDNA ends

Rapid amplification of cDNA ends (RACE) experiments were conducted using the Smarter RACE cDNA Amplification kit (Clontech). Briefly, at least two sets of primers were designed and synthesized for 5′RACE, 3′RACE and their matching nested PCR (Supplementary Table S1). The PCR products were isolated by 1.0% agarose gel electrophoresis and were purified utilizing a Gel Extraction Kit (CWBIO). The target fragment was cloned into a pMD18-T PCR cloning vector (Takara) for sequencing.

Northern blot assay

The DIG Northern Starter Kit (Roche Applied Science) was employed to detect expression of HCCL5 following the manufacturers' protocol. The chemiluminescent signal generated by the CDP-Star (Roche Applied Science). The substrate was tested by exposure of the membranes to the ChemiDoc MP System (Bio-Rad). A GAPDH probe was end labeled as the control. The exposure time for HCCL5 and GAPDH was 30 minutes. The probe sequences are provided in Supplementary Table S2.

Construction of vectors for HCCL5 full-length overexpression and shRNA

The full-length of human HCCL5 was amplified via RT-PCR (Supplementary Table S3), with cDNA of HepG2 being used as amplification template. The PCR product and pcDNA3.1 (+) vector were digested by *Hin*dIII (restriction site: AAGCTT) and *Xho*I (restriction site: CTCGAG) restriction enzymes (Thermo Fisher Scientific) at 37°C for 1 hour, and ligated by T4 ligase (Thermo Fisher Scientific) at 22°C for overnight. The recombinant vector for overexpression of HCCL5 was validated by Sanger sequencing.

Four shRNA plasmids (L5-shRNA 1–4) targeting HCCL5 and one scramble control shRNA (shNC) were constructed into either pGPU6/GFP/Neo or pLKO.1 shRNA expression vector by Shanghai GenePharma Company. Primer sequences used for cloning were provided in Supplementary Table S3. The pGPU6/GFP/Neo vector designed for the cloning and stable expression of shRNA in mammalian cells is under the control of human U6 promoter.

Cell proliferation assay

Cells were seeded at 1,000 cells per well in 96-well plates with 100 μL of RPMI1640 medium. Cell Counting Kit-8 (CCK-8) Assay Kit (Dojindo) was applied to measure cell proliferation daily for a consecutive of 7 days. For colony formation assay, 200–1,000 cells were seeded into 6-well plate. After 10–15 days, colonies were stained with 0.1% crystal violet (DINGGUO) and counted. Cells were maintained in RPMI1640 supplemented with low concentration (0.1%–5%) of FBS.

Flow cytometry analysis

In cell-cycle analysis, cells were collected and fixed in ice-cold 70% ethanol at 4°C overnight, followed by rinsing with D-Hanks, and incubated with 100 μL of propidium iodide (PI) staining solution (Genview) containing PI (50 μg/mL) and RNase A (20 μg/mL). Apoptosis analysis was performed using Annexin V-FITC/PI Apoptosis Detection Kit (TransGen Biotech). Flow cytometry data were analyzed using the ModFit software (Verity Software House).

Wound-healing assay

Cells were seeded into 6-well plates, and the cell monolayer was wounded by sterile 100-μL pipette tips when cells reached approximately 90% confluence. Cells were then rinsed three times with D-Hanks to wipe off the detached cells and were incubated in RPMI1640 containing 5% FBS for 48 hours. At both 0 and 48 hours, cell scratches were photographed under an inverted microscope (200×), and the gap size was measured and calculated by ImageJ.

Transwell migration and invasion assays

For migration assay, cells were plated into the top chamber (8 μm; Corning; catalog no.: 3422). For invasion assay, cells were added into the top chamber precoated with Matrigel (Matrigel Basement Membrane Matrix; BD Biosciences; catalog no.: 354234). The bottom chamber was filled with DMEM or RPMI1640 supplemented with 20% FBS. The membranes were incubated for 24–48 hours and then were stained with 0.1% crystal violet for 10 minutes. The numbers of migrated and invaded cells on lower surface of the membrane were calculated using a microscope (Olympus).

Tumor xenograft assay in nude mice

Tumor xenograft assay was performed as described previously (31). Briefly, SMMC-7721 cells (5×10^6 cells per mouse) stably transfected with indicated vectors were injected subcutaneously into 4-week old BALB/c male nude mice (8 nude mice for each group). The tumor dimensions were measured every two days. Mice in all groups were sacrificed by cervical dislocation after 30 days. Xenograft tumors were weighed, fixed in 4% paraformaldehyde, and embedded in paraffin for Ki-67 and TdT-mediated dUTP nick end labeling (TUNEL) staining. The tumor size was calculated using the following formula: Tumor volume (mm^3) = length (mm) × width^2 (mm^2) × π/6. The images of Ki-67 and TUNEL staining were qualified by Image-Pro Plus software. The experimental protocols were approved by the Ethics Committee of Xiangya Hospital of Central South University (Changshu, P.R. China).

Western blotting

Western blotting experiment was performed as described previously (32). The following primary antibodies were used: E-cadherin (1:1,000; Cell Signaling Technology), ZO-1 (1:1,000; Cell Signaling Technology), N-cadherin (1:1,000; Cell Signaling Technology), vimentin (1:1,000; Cell Signaling Technology), Snail (1:500; Cell Signaling Technology), Slug (1:500; Cell Signaling Technology), TCF8/ZEB1 (1:500; Cell Signaling Technology), Twist1 (1:1,000; Abclonal), and β-actin (1:3,000; TransGen Biotech). All bands of Western blot analysis were qualified by ImageJ software.

Immunofluorescence analysis

HCC cells were fixed with 4% paraformaldehyde, followed by the incubation with primary antibodies against E-cadherin (1:200; Cell Signaling Technology), N-cadherin (1:200; Cell Signaling Technology), or vimentin (1:100; Cell Signaling Technology) overnight at 4°C. Cells were subsequently incubated with Cy3-conjugated secondary antibody for 30 minutes at room temperature. The nuclei were finally stained with DAPI for 3 minutes. The images were acquired using fluorescence microscopy (Nikon Corporation) and were qualified by Image-Pro Plus software.

In situ hybridization assay

In situ hybridization (ISH) probes (1: 5′- ACCTA CAGAG TATGA TTATT CATCT TTACA TTGCC -3′; 2: 5′- TCTAG ACCTT TGCTT GTGTT GTTTG TTCTC TGCCT -3′; 3: 5′- CTTCC AGACC AGTTT GGTGG TGCCC CTAAT CCACA -3′) for the detection of digoxin-labeled HCCL5 was designed and synthesized by BOSTER (Boster Biological Technology Ltd.). Two commercial HCC tissue arrays (Discovery and Validation set) were purchased from OUTDO (SHANGHAI OUTDO BIOTECH CO.) and AURAGENE (AURAGENE BIOTECH). The staining score of HCCL5 was evaluated to be either 0 (negative) or 1 (positive) by two independent pathologists.

Survival analysis

The most updated (September 2018) HCC datasets were downloaded from The Cancer Genome Atlas (TCGA; https://cancergenome.nih.gov/), wherein a total of 371 tumor samples and 50 nonmalignant liver tissues are included. TCGA HCC patients were classified into HCCL5-high and HCCL5-low groups by the median expression level of HCCL5. Similarly, the median value of ZEB1 mRNA level was applied to stratify TCGA samples into ZEB1-high and ZEB1-low groups. All survival-related plots were plotted using GraphPad software. A two-sided $P < 0.05$ was considered as statistically significance.

Chromatin immunoprecipitation sequencing and ChIA-PET data analysis

Chromatin immunoprecipitation sequencing (ChIP-seq) data (ZEB1, pol2, H3K4me1, H3K4me3, and H3K27ac) of HepG2 cell line was obtained from Encyclopedia of DNA Elements (ENCODE) database (https://www.encodeproject.org/). The Rank Ordering of Super Enhancers (ROSE) algorithm (33) was used to compute and identify superenhancer from H3K27ac ChIP-seq data. The bigwig files of ZEB1, pol2, H3K4me1, H3K4me3, and H3K27ac were visualized via Integrative Genomics Viewer (IGV).

The raw Chromatin Interaction Analysis by Paired-End Tag (ChIA-PET) sequencing data (ENCLB951KEQ and ENCLB607ZTO) in HepG2 cell line was downloaded from ENCODE database. The sequencing data of two-biological duplicates was first merged. To identify chromatin loops, we processed the data by ChIA-PET2 (https://github.com/GuipengLi/ChIA-PET2) using parameters -e 1 -k 2. Specifically, we performed the following steps with ChIA-PET2: linker trimming, read alignment, duplicate removal, peak calling, and chromatin loop calling. Finally, the identified chromatin loops were visualized by WASHU EPIGENOME BROWSER (http://epigenomegateway.wustl.edu/browser/).

Dual-luciferase reporter assay

The superenhancer of HCCL5 was divided into five components (E1–E5) and was constructed to pGL3-promoter vector (Supplementary Table S4). HCC cells (HepG2, SMMC-7721 and HCCLM3) were counted and plated in 6-well dishes. Cells were transfected with Lipofectamine 2000 (Invitrogen) with 2.5 μg vectors (pGL3-promoter, NC, E1, E2, E3, E4, and E5), and 250 ng pRL-TK as internal control. After 48 hours, the luciferase activities of each group were detected using Dual-Luciferase Reporter Assay System (Promega). The ratio of luciferase activities in firefly to those in *Renilla* was normalized against the pGL3-promoter vector.

ChIP-qPCR

ChIP for ZEB1 was performed using the protocol described previously (24, 31, 34). Briefly, HCC cells were cross-linked with a final concentration of 1% formaldehyde (Sigma-Aldrich), and were quenched by a final concentration of 125 mmol/L glycine. After cells were lysed, cold shearing buffer containing protease inhibitors (Roche Applied Science) was added, and then the chromatin was sheared through sonication to obtain fragment sizes 150–1,000 bp. The antibody against ZEB1 (ProteinTech) and normal rabbit IgG (Cell Signaling Technology) were used for immunoprecipitation. qPCR (primers were shown in Supplementary Table S5) was conducted to measure the enrichment of ZEB1 on DNA molecules of interest.

Statistical analysis

All statistical data were displayed as means ± SD and were analyzed using SPSS 17.0 (IBM). The significance of the differences between two groups analyzed with Student *t* test, while the differences among three or more groups was conducted by using one-way ANOVA. Differences between the clinicopathologic data of HCCL5-high and HCCL5-low patients were analyzed using the χ^2 test. All plots were drawn by using GraphPad Prism 5.0 Software (*, $P < 0.05$; **, $P < 0.01$; ***, $P < 0.001$).

Results

In silico analysis identified noncoding ESTs expressed in HCC

As an effort to identify noncoding transcripts expressed specifically in HCC tissues, we analyzed EST libraries from liver cancer samples and nonliver tumor samples using CGAP database (see Materials and Methods). Upon removing coding transcripts, repetitive elements, and intron-less ESTs, we identified five novel candidate EST fragments (L1–L5) expressed uniquely in liver cancer samples compared with other tumor types. We next measured the mRNA levels of L1–L5 in HepG2 cells by RT-PCR, and identified that L5 was expressed at the highest level (Supplementary Fig. S1A).

HCCL5 is an uncharacterized cytoplasmic lncRNA in HCC cells

As transcript L5 (here and after designated as HCCL5) was more conspicuous in RT-PCR validation, we next performed 3′ RACE and 5′ RACE to identify its full sequence (Supplementary Fig. S1B and S1C). An 823-bp sequence was determined and its expression was confirmed by Northern blotting (Supplementary Fig. S1D). *HCCL5* gene consists of two exons (Supplementary Fig. S1E), and our RACE results showed that it was an extension of the uncharacterized *LOC105371083* (715 bp, Refseq database; Ensembl: ENSG00000263080; Ensembl version: ENSG00000263080.1).

Coding potential calculator (CPC) predicted that HCCL5 had no effective open reading frame (ORF) and it could not encode peptides (Supplementary Fig. S1F). The lack of protein-coding potential of HCCL5 was further confirmed by ORF Finder (Supplementary Fig. S1G), characterizing HCCL5 as a long noncoding RNA (lncRNA). Supportively, no conserved domains in HCCL5 sequence were identified by either Conserved Domains Database (CDD) or Pfam 28.0 analysis (Supplementary Fig. S1H and S1I).

We next performed the nuclear/cytosol fractionation experiment to determine the subcellular localization of HCCL5. With validating the nuclear/cytosol fractionation successfully, lncRNA MALAT1 was located in the nucleus (35–38), while both MT-CO1 mRNA (Mitochondrially Encoded Cytochrome C Oxidase I) and GAPDH mRNA were mainly located in the cytoplasmic faction. Importantly, the majority of HCCL5 was distributed in cytoplasm (Supplementary Fig. S2).

HCCL5 enhances the malignant phenotypes of HCC cells

To explore the biological functions of HCCL5 in HCC cells, the HepG2, SMMC-7721, and HCCLM3 cell lines were chosen for experiments (Supplementary Fig. S3), and both gain-of-function and loss-of-function assays were conducted. We first validated the efficiency of both overexpression (Supplementary Fig. S4A and S4B) and silencing of HCCL5 (Supplementary Fig. S4C–E) via qRT-PCR. Importantly, overexpression of HCCL5 potently accelerated the growth of HCC cell lines (Fig. 1A and B), while HCCL5 silencing produced the opposite effect (Fig. 1C and D). These results are consistent with colony growth assay (Supplementary Fig. S5A–S5D), demonstrating that HCCL5 promotes the proliferation of HCC cells.

Flow cytometric analysis demonstrated that overexpression of HCCL5 led to a significant reduction of cells at G_0–G_1 phase (Supplementary Fig. S6A–S6D) and an accumulation of cells in S-phase (Supplementary Fig. S6A and S6B), while HCCL5 silencing displayed the opposite effect (Supplementary Fig. S6E and S6F). Yet, HCCL5 overexpression (Supplementary Fig. S7A–S7D) or silencing (Supplementary Fig. S8A–S8D) did not regulate cell death of HCC cells. The effect of HCCL5 on HCC cell motility was determined next. In both wound healing and Transwell assays, cell migratory and invasive capabilities were enhanced by forced expression of HCCL5 (Fig. 1E–H; Supplementary Fig. S9A and S9B), and they were significantly impaired by HCCL5 depletion (Fig. 1I–L; Supplementary Fig. S9C and S9D).

To further evaluate the function of HCCL5 in HCC growth, *in vivo* xenograft assay was performed. In agreement with the above *in vitro* results, a significant increase of proliferation was found in SMMC-7721 xenograft with HCCL5 overexpression compared with the control group (Fig. 2A and B). In contrast, HCCL5 silencing reduced the growth of xenograft (Fig. 2C and D). Furthermore, larger proportions of cells were positive for Ki-67 staining in the HCCL5-overexpressed group relative to that in the control group (Fig. 2E; Supplementary Fig. S10A). Supportively, knockdown of HCCL5 resulted in fewer Ki-67–positive cells (Fig. 2F; Supplementary Fig. S10B). In addition, TUNEL staining analysis showed that HCCL5 overexpression had no effect on cell apoptosis (Fig. 2G; Supplementary Fig. S10C), while HCCL5 depletion promoted cell apoptosis of HCC cells *in vivo* (Fig. 2H; Supplementary Fig. S10D). Collectively, these results highlight HCCL5 as a novel oncogenic lncRNA in HCC cells.

HCCL5 is upregulated by TGF-β1 and promotes EMT process

We next sought to probe molecular mechanisms underlying the oncogenic functions of HCCL5. In a separated project to profile TGF-β1-regualted lncRNAs during EMT (manuscript under preparation), we accidently noted that HCCL5 was also strongly induced by TGF-β1 treatment (Fig. 3A–C). Given the importance of EMT in cancer biology, we next tested the function of HCCL5 in this process. Real-time PCR, Western blotting, and immunofluorescence assays all consistently showed that HCCL5 overexpression decreased the abundance of epithelial markers (E-cadherin and ZO-1) and elevated the level of mesenchymal markers (N-cadherin and vimentin; Fig. 3D–F; Supplementary Fig. S11A and S11B). Conversely, HCCL5 silencing generated the opposite alterations (Fig. 3G–J; Supplementary Fig. S11C and S11D).

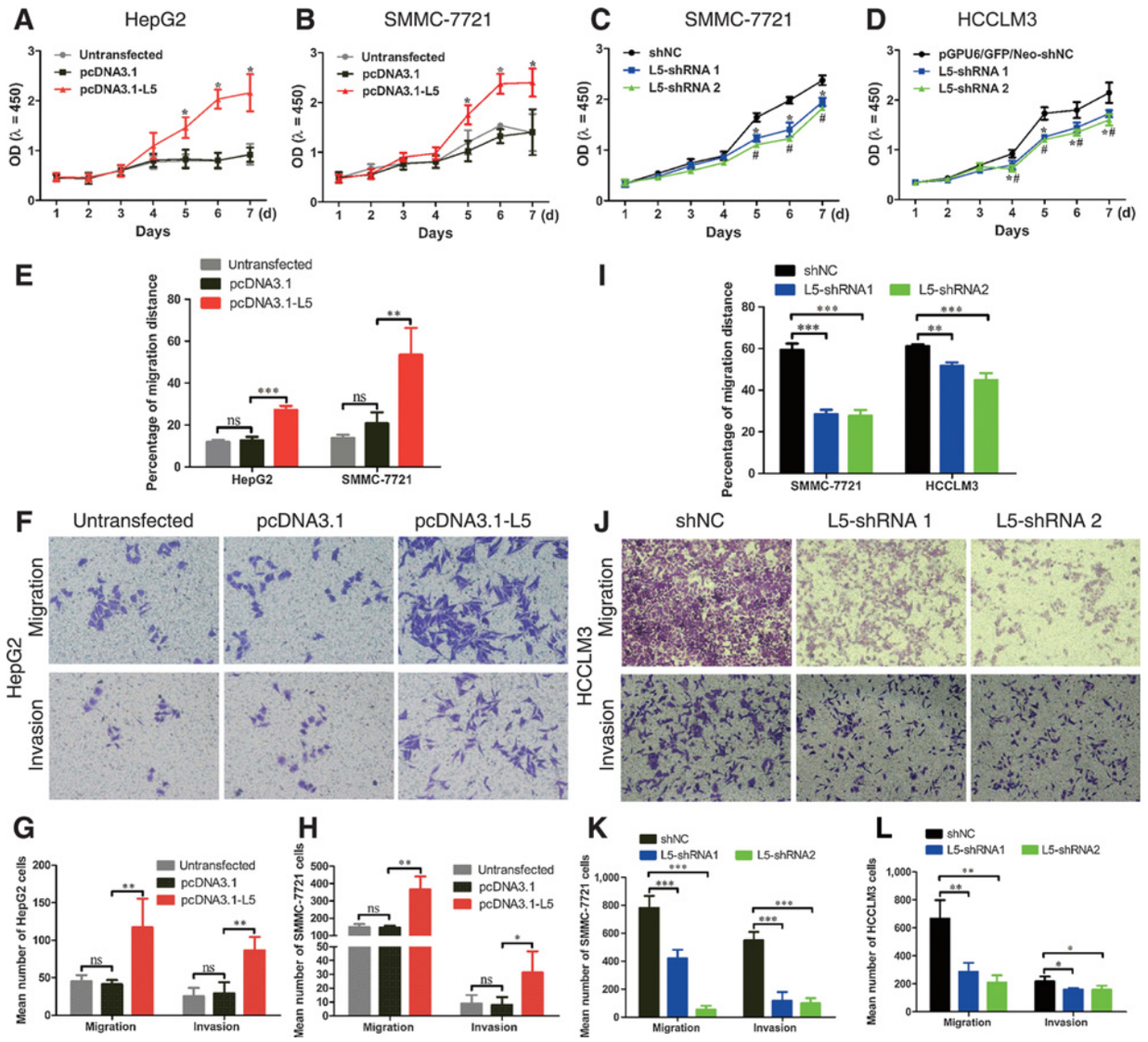

Figure 1.

HCCL5 enhances cell viability, migration, and invasion of HCC cells. **A** and **B,** The effects of lncRNA HCCL5 overexpression on the proliferation of HepG2 and SMMC-7721 cell lines. **C** and **D,** The effects of HCCL5 knockdown on the proliferation of SMMC-7721 and HCCLM3 cell lines. **E,** The effects of HCCL5 overexpression on the motility in HCC cells were examined by wound-healing assay. **F–H,** The effects of HCCL5 overexpression on cell migration and invasiveness in HCC cells were examined by Transwell assays using a Boyden chamber in the presence or absence of Matrigel, respectively. **I,** The effects of HCCL5 silencing on the motility in HCC cells were examined by wound-healing assay. **J–L,** The effects of HCCL5 overexpression and silencing on cell migration and invasiveness in HCC cells were examined by Transwell assays using a Boyden chamber in the presence or absence of Matrigel, respectively. Data are representative of 2–3 separate experiments performed in triplicate. *, $P < 0.05$; **, $P < 0.01$; ***, $P < 0.001$; ns, nonsignificant.

We next conducted survival analysis using TCGA HCC cohort, and found that patients with HCC with higher E-cadherin expression had significantly better overall survival (HR = 0.6317; 95% CI = 0.4409–0.9050; $P < 0.05$) and 5-year survival (HR = 0.6061; 95% CI = 0.4222–0.8702; $P < 0.01$) than those with lower E-cadherin expression (Supplementary Fig. S12A B). There was no difference of overall survival or 5-year survival between higher vimentin expression and lower vimentin expression (Supplementary Fig. S12C and S12D). Moreover, an unfavorable overall survival (HR = 2.453; 95% CI = 1.536–3.917, $P <$ 0.001) and 5-year survival (HR = 2.384; 95% CI = 1.496–3.799, $P < 0.001$) were observed in patients with HCC with the combination of high vimentin and low E-cadherin expression (Supplementary Fig. S12E and S12F). These data supported the findings and significance of HCCL5 in HCC.

Considering these changes, the levels of EMT-related transcription factors were next measured. In agreement with the cellular phenotypical results, HCCL5 overexpression increased the amount of EMT-promoting transcription factors, including Snail, Slug, ZEB1, and Twist1 (Fig. 4A–C), and all of which were reduced

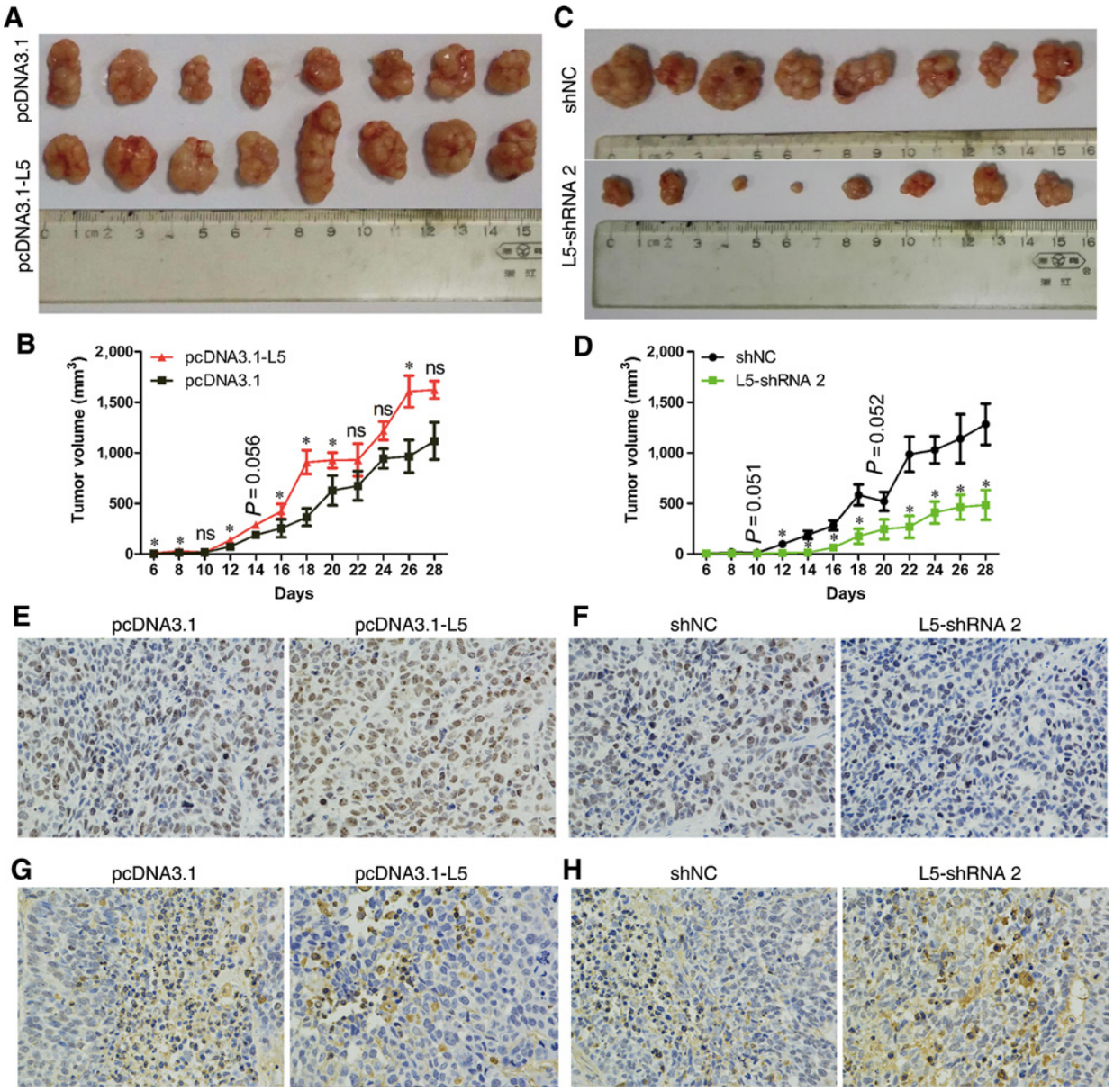

Figure 2.

HCCL5 promotes xenogeneic growth of HCC cells *in vivo*. **A** and **C,** HCC cells SMMC-7721 stably transfected with indicated vectors (pcDNA3.1, pcDNA3.1-L5, shNC, and L5-shRNA 2) were injected subcutaneously into 4-week-old BALB/c male nude mice (8 nude mice for each group). Representative images of dissected xenogeneic tumors from nude mice in each group. **B** and **D,** Tumor volumes were measured and calculated every two days following the subcutaneous injection. Tumor tissues were subjected to Ki-67 staining (**E** and **F**) and TUNEL staining (**G** and **H**). All staining images are displayed at ×400. ns, nonsignificant.

upon HCCL5 silencing (Fig. 4D–G; Supplementary Fig. S13). These data together suggest that HCCL5 plays a prominent role in the promotion of EMT in HCC cells, through regulating the expression of master EMT-related transcription factors.

Overexpression of HCCL5 in human HCC tissues

We next examined HCCL5 expression by *in situ* hybridization in a discovery set ($n = 15$ pairs) of human HCC tissues, and found that the positive expression rate of HCCL5 in HCC was significantly higher than that in adjacent nonmalignant tissues (Fig. 5A). In an independent validation set with larger number of cases ($n = 196$), overexpression of HCCL5 in HCC was confirmed (Fig. 5B–E). Notably, the level of HCCL5 was further elevated in metastatic HCCs compared with primary tumors (Fig. 5E). The clinicopathologic characteristics of discovery set ($n = 15$ pairs) and validation set ($n = 196$) were shown in Supplementary Data (Supplementary Table S6–S9). Further confirming our results, a strong and significant upregulation of HCCL5 was noted in HCC primary tumors from TCGA RNA-seq data (Fig. 5F). Importantly, an unfavorable overall survival and 5-year survival were observed

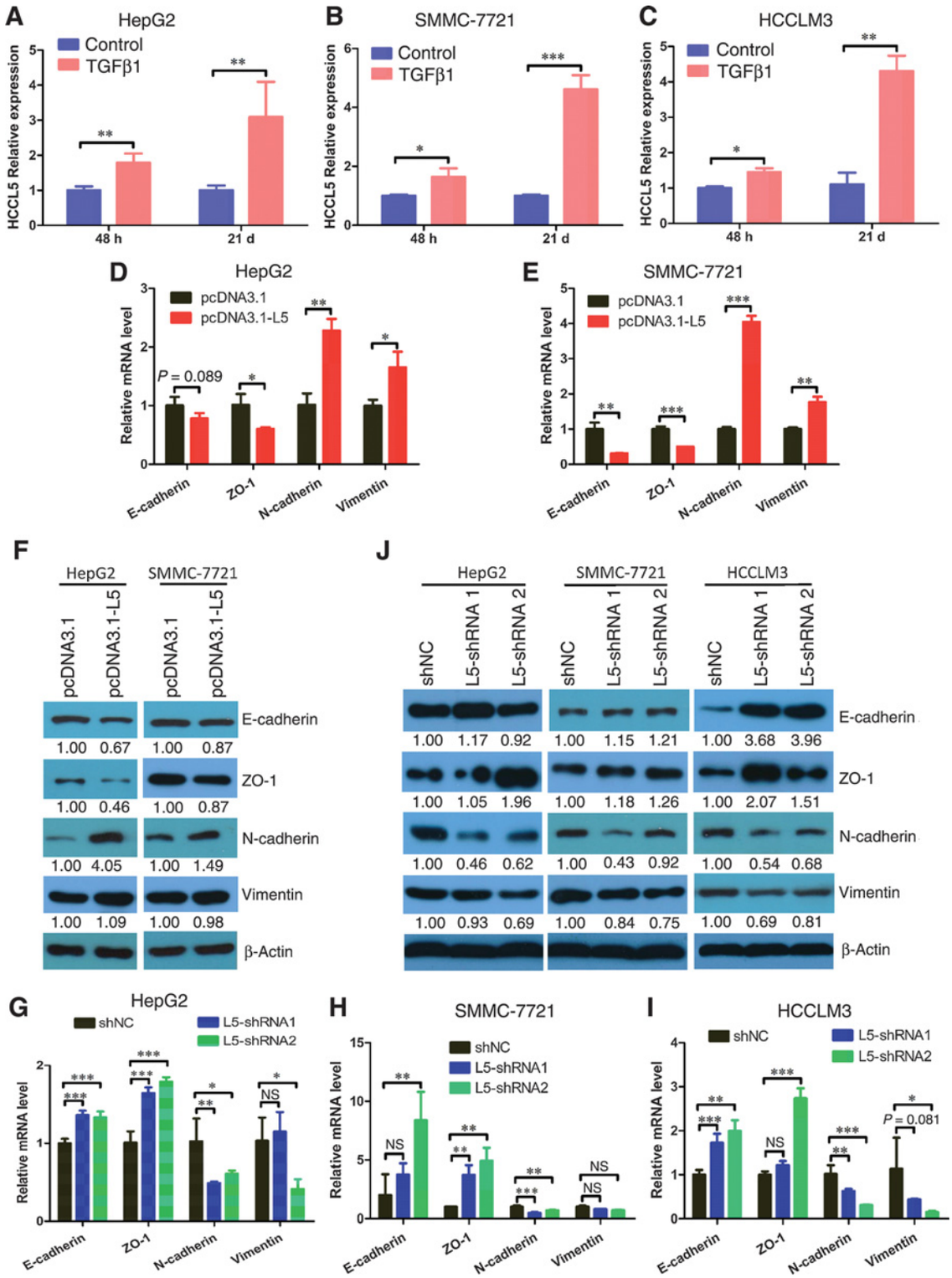

Figure 3.

TGF-β1-induced HCCL5 promotes EMT of HCC cells. **A–C,** The expression of HCCL5 upon the treatment of TGF-β1 (10 ng/mL) for 48 hours or 21 days in HepG2 (**A**), SMMC-7721 (**B**), and HCCLM3 cells (**C**). Relative mRNA expression (**D** and **E**) and the protein level of EMT markers (E-cadherin, ZO-1, N-cadherin and vimentin; **F**) in HCC cells stably overexpressing HCCL5. Relative mRNA expression (**G–I**) and the protein level of EMT markers (E-cadherin, ZO-1, N-cadherin, and vimentin; **J**) in HCC cells stably expressing HCCL5 shRNA vectors. Data are representative of 2–3 separate experiments. *, $P < 0.05$; **, $P < 0.01$; ***, $P < 0.001$; NS, nonsignificant.

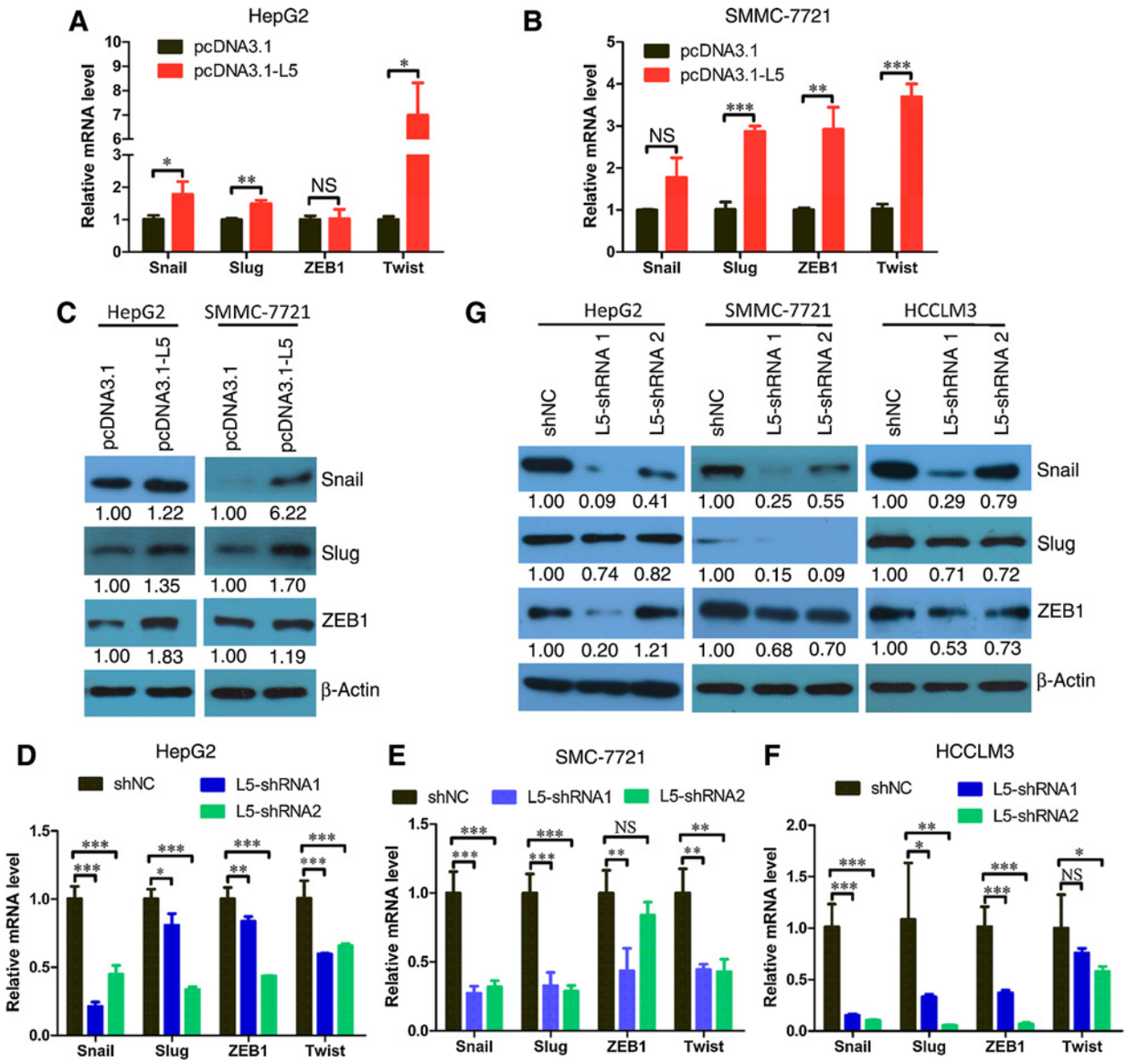

Figure 4.

HCCL5 upregulates the expression of EMT-associated transcription factors in HCC cells. **A** and **B,** The mRNA expression of EMT-associated transcription factors Snail, Slug, ZEB1, and Twist in HCC cells stably expressing HCCL5 overexpression vectors. **C,** The protein expression of EMT-associated transcription factors Snail, Slug, and ZEB1 in HCC cells stably expressing HCCL5 overexpression and shRNA vectors. β-Actin served as an internal control. **D–F,** The mRNA expression of EMT-associated transcription factors Snail, Slug, ZEB1, and Twist in HCC cells stably expressing HCCL5 shRNA vectors. **G,** The protein expression of EMT-associated transcription factors Snail, Slug, and ZEB1 in HCC cells stably expressing HCCL5 shRNA vectors. β-Actin served as an internal control. Data are representative of 2–3 separate experiments. *, $P < 0.05$; **, $P < 0.01$; ***, $P < 0.001$; NS, nonsignificant.

in patients with HCC with high HCCL5 expression (Fig. 5G and H).

Superenhancer-associated HCCL5 is transcriptionally activated by ZEB1 in HCC

Considering the upregulation of HCCL5 in HCC tissues and its induction during EMT, we next investigated the transcriptional regulation of this lncRNA. Analysis of H3K27ac ChIP-seq data generated in HepG2 cells identified a superenhancer 18-kb downstream of HCCL5 (Fig. 6A). The active nature of this superenhancer was corroborated by the cooccupancy of both pol2 and H3K4me1 (Fig. 6A). Furthermore, ChIA-PET data from HepG2 cells highlighted that this superenhancer had direct interactions with the promoter region of HCCL5 (Fig. 6B). Notably, ZEB1 bound to both the identified superenhancer and promoter of HCCL5, and the occupancy aligned with both H3K27ac and pol2 binding. Importantly, silencing of ZEB1 significantly decreased HCCL5 expression (Fig. 6C–E). Moreover, knockdown of ZEB1

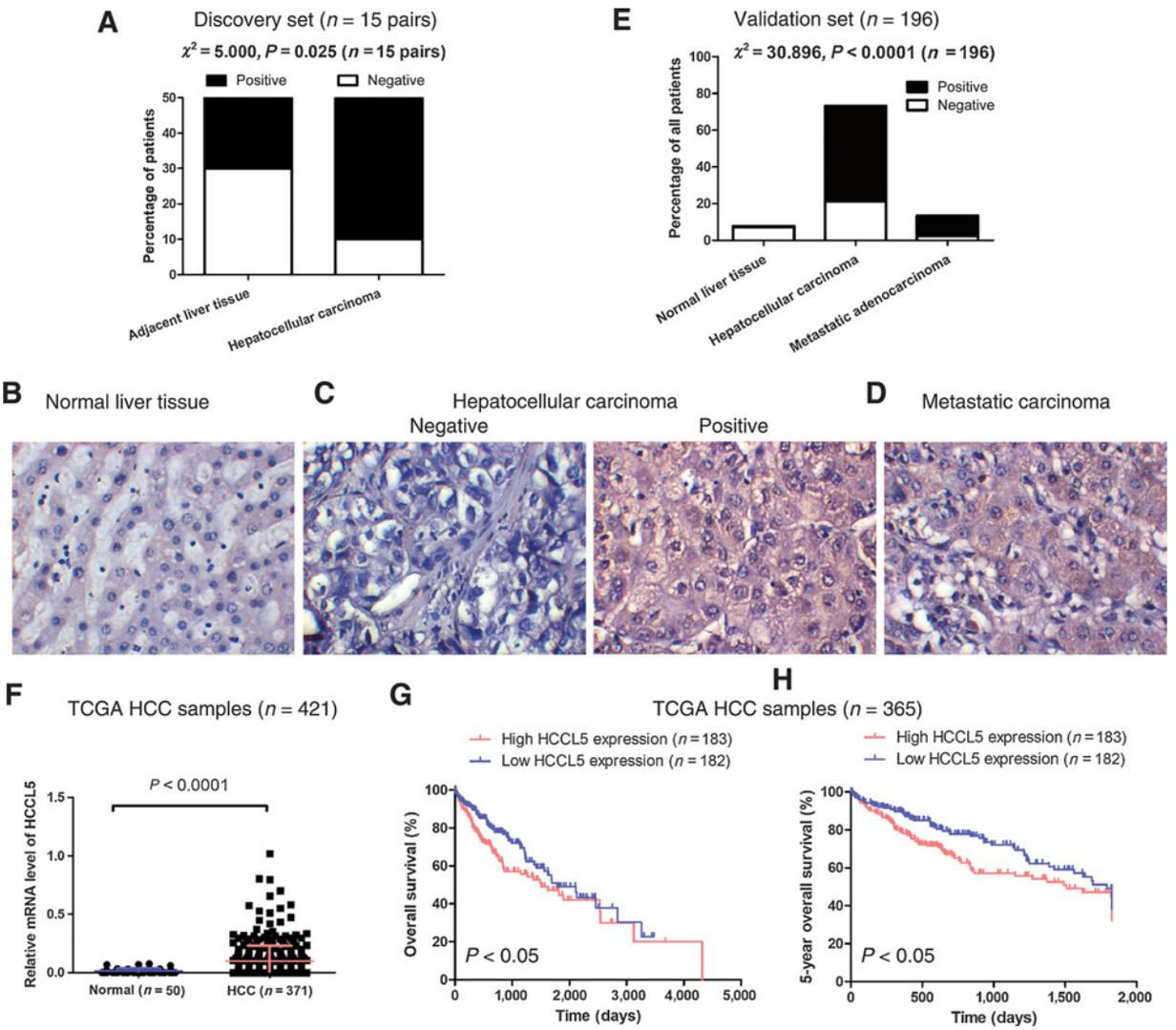

Figure 5.

HCCL5 expression was upregulated in human HCC tissues. **A,** Bar plots showing HCCL5 expression in HCC samples and matched nonmalignant liver tissues in a discovery set ($n = 15$ pairs). **B–D,** Representative images of *in situ* hybridization staining (×400). **E,** Bar plots showing HCCL5 expression in a validation set ($n = 196$). **F,** Scatter plots showing HCCL5 expression in HCC samples and normal liver tissues in TCGA dataset. **G** and **H,** Overall survival of TCGA HCC patients stratified on the basis of the expression of HCCL5. The HCC dataset was downloaded from TCGA (https://cancergenome.nih.gov/).

reduced TGF-β1-induced HCCL5 level (Fig. 6F and G). In addition, high ZEB1 expression was significantly correlated with poor overall survival of patients with HCC (Fig. 6H).

The superenhancer of HCCL5 was further divided into five constituents (E1–E5) and was constructed into pGL3-promoter vector for luciferase reporter assay. Importantly, compared with negative control DNA segment, the enhancer activity of E3 and E4 was significantly higher in HCC cells (Fig. 7A–D), but not in 293T cells (Supplementary Fig. S14), which were reduced by silencing of ZEB1 in HCC cells (Fig. 7E–G). Furthermore, ChIP-qPCR results showed that ZEB1 specifically bound to E3 and E4 within HCCL5 superenhancer (Fig. 7A, H–J), verifying the ChIP-Seq data. These data demonstrate that ZEB1 interacts with both superenhancer and promoter regions of HCCL5 and enhances its transcription in both steady-state and EMT process.

Discussion

In this study, we identify an uncharacterized lncRNA, HCCL5, as a novel oncogenic factor promoting the growth, invasion, and metastasis of HCC cells both *in vitro* and *in vivo*. The expression of HCCL5 was upregulated in TGF-β1-induced EMT model. Mechanistically, ZEB1 directly bound superenhancer and promoter region of HCCL5, and activated the transcription of this lncRNA. Functionally, HCCL5 accelerates the EMT phenotype in HCC cells by elevating the abundance of transcription factors Snail, Slug,

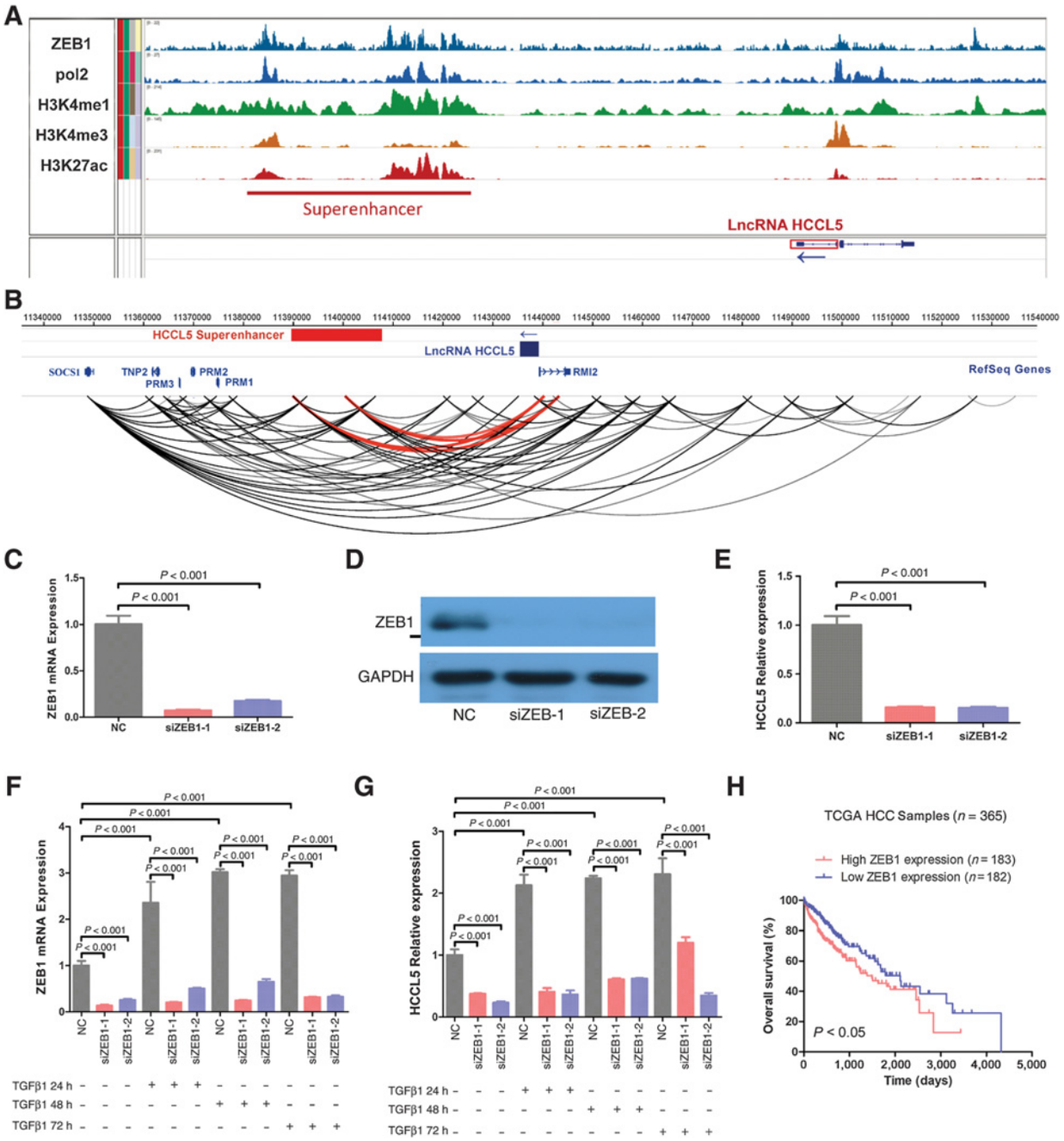

Figure 6.

ZEB1 interacted with both HCCL5 super-enhancer and promoter region and promoted its transcription. **A,** ChIP-seq profiles of indicated histone markers, pol2 and ZEB1 in HepG2 cells. **B,** ChIA-PET data showing the interaction between the promoter region of HCCL5 and its super-enhancer in HepG2 cells. Results from **A** and **B** were reanalyzed on the basis of Encode project (https://www.encodeproject.org/). **C–E,** qRT-PCR and Western blot assays measuring the expression of HCCL5 upon silencing of ZEB1 in SMMC-7721 cells in the absence or presence (**F** and **G**) of TGF-β1 (10 ng/mL) treatment for various periods of time (24, 48, and 72 hours). **H,** Overall survival of TCGA HCC patients stratified on the basis of the expression of ZEB1. The HCC dataset was downloaded from TCGA (https://cancergenome.nih.gov/). Data of **C–G** are representative of 2–3 separate experiments.

ZEB1, and Twist1. Finally, a strong upregulation of HCCL5 was noted in HCC primary tissues.

EMT is a key process responsible for cancer metastasis, which is a major cause of the high mortality and poor survival of patients with HCC (39–42). EMT is characterized by the loss of epithelial cell polarity and cell adhesion with the acquisition of mesenchymal-like features, leading to increased cell migration and invasion (43–45). The functional relationship between TGF-β signaling

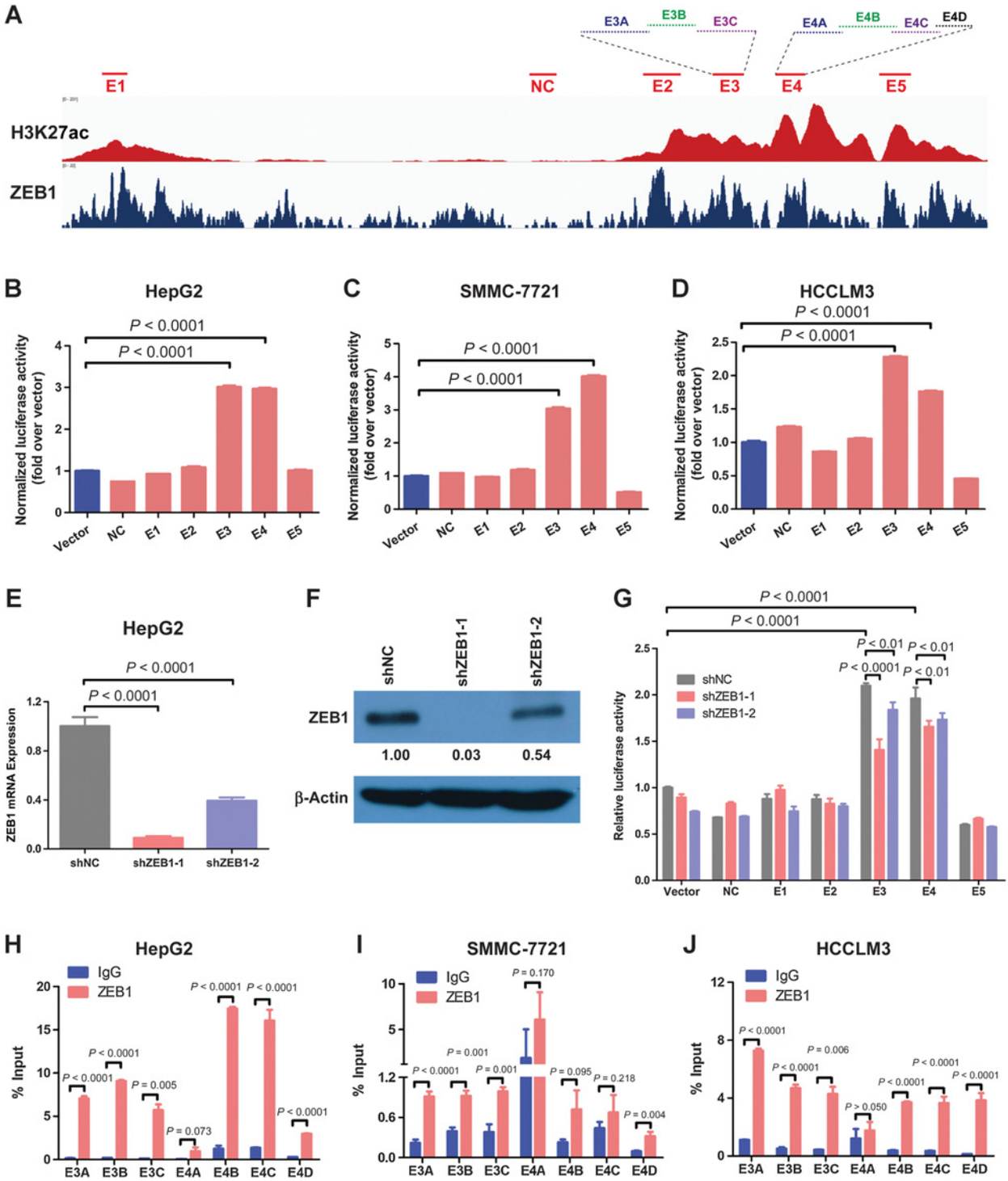

Figure 7.

ZEB1 directly bound to super-enhancer of HCCL5. **A,** Five constituent enhancers (E1–E5) within the super-enhancer were cloned into luciferase reporter vector pGL3-promoter. E3 and E4 segment were, respectively, divided into three (E3A, E3B, and E3C) and four constituents (E4A, E4B, E4C, and E4D) for ChIP-qPCR. **B–D,** The luciferase activities of these five enhancer elements were measured through Dual-Luciferase Reporter Assay in HepG2, SMMC-7721, and HCCLM3. **E** and **F,** The knockdown efficiency of ZEB1 was measured by qRT-PCR and Western blot analysis. **G,** The luciferase activities of these five enhancer elements were determined through Dual-Luciferase Reporter Assay in HepG2 cells upon ZEB1 silencing. **H–J,** The interaction between ZEB1 and the constituents of superenhancer was detected by ChIP-qPCR analysis in HepG2, SMMC-7721, and HCCLM3. Rabbit normal IgG antibody was used as a negative control. Data are representative of 2–3 separate experiments.

and EMT is well-characterized, but the biological involvement of lncRNAs in this process was not completely understood. Several notable examples, including ANCR (46), Lnc-Spry1 (47), LINC01186 (48), LINC01133 (49), and lncRNA-ATB (50), were found to mediate TGF-β-induced EMT in breast cancer and other cancers.

Integrative analysis of ChIP-seq and ChIA-PET data in HepG2 cells identified a superenhancer physically interacting with the promoter region of HCCL5. Functionally, superenhancers often drive the expression of key factors that control cell identity, and thus they play important roles in the pathogenesis of different diseases including cancer (21, 33, 51). A close relationship between superenhancer and miRNA expression was recently discovered (22). Yet, how superenhancer regulates lncRNAs has not been expensively investigated. In this study, we demonstrated that ZEB1, a TGF-β1-inducible EMT transcription factor, bound directly to HCCL5 superenhancer and activated its transcription in HCC cells.

We also demonstrated that HCCL5 functionally promoted EMT through increasing the expression of a few EMT-associated transcription factors, including Snail, Slug, ZEB1, and Twist1. Multiple additional lncRNAs, such as CARLo-5 (52), MALAT1 (53), Unigene56159 (52), and lncRNA-ATB (54), were reported to accelerate EMT process or tumor progression of HCC via functioning as sponges to compete with miRNAs. As our results showed that the majority of HCCL5 was located in cytoplasm, we speculate that HCCL5-mediated upregulation of these EMT-associated transcription factors is through indirect mechanisms, which needs to be characterized in future studies.

The overexpression of HCCL5 was validated in two independent HCC cohorts by *in situ* hybridization assay. Using TCGA RNA-seq data, we confirmed the upregulation of HCCL5 in HCC primary tumors. Furthermore, high HCCL5 expression predicted a poor overall survival and 5-year overall survival in patients with HCC. These results support the oncogenic role of HCCL5 identified in our current study and highlight its potential clinical significance in HCC. In summary, our study uncovers a novel functional lncRNA promoting HCC malignancy and also provides insights into the transcriptional regulation of EMT. Furthermore, upregulation of HCCL5 in human HCC has potential to serve as a novel biomarker for this deadly disease.

Disclosure of Potential Conflicts of Interest

No potential conflicts of interest were disclosed.

Authors' Contributions

Conception and design: L. Peng, D. Yin, G. Li, D.-C. Lin
Development of methodology: L. Peng, B. Jiang, X. Yuan, Y. Qiu, J. Peng, Y. Huang, C. Zhang, C. Li
Acquisition of data (provided animals, acquired and managed patients, provided facilities, etc.): G. Li
Analysis and interpretation of data (e.g., statistical analysis, biostatistics, computational analysis): L. Peng, Z. Lin, J. Li, Y. Zhang, M. Meng, X. Pan, C. Li, X. Bi, G. Li, D.-C. Lin
Writing, review, and/or revision of the manuscript: L. Peng, X. Yuan, D.-C. Lin
Administrative, technical, or material support (i.e., reporting or organizing data, constructing databases): Y. Zhang, W. Yao, W. Deng, X. Bi, G. Li
Study supervision: G. Li, D.-C. Lin

Acknowledgments

We are grateful for ChIP-seq and ChIA-PET data from ENCODE database, and for the HCC dataset from TCGA project team. This work was supported by the National Natural Science Foundation of China (grant no. 81802812 to L. Peng), the Natural Science Foundation of Guangdong Province (grant no. 2018A030313129 to L. Peng), Hunan Provincial Innovation Foundation for Postgraduates (grant no. CX2016B056 to L. Peng), the Open-End Fund for the Valuable and Precision Instruments of Central South University (grant no. CSUZC201746 to L. Peng), Fundamental Research Funds for the Central Universities of Central South University (grant no. 2015zzts096 to L. Peng), and the Science and Technology Department Research Foundation of Hunan province (grant no. 12JJ2052 to G. Li).

The costs of publication of this article were defrayed in part by the payment of page charges. This article must therefore be hereby marked *advertisement* in accordance with 18 U.S.C. Section 1734 solely to indicate this fact.

Received February 2, 2018; revised August 1, 2018; accepted November 21, 2018; published first November 27, 2018.

References

1. Ferlay J, Soerjomataram I, Dikshit R, Eser S, Mathers C, Rebelo M, et al. Cancer incidence and mortality worldwide: sources, methods and major patterns in GLOBOCAN 2012. Int J Cancer 2015;136:E359–86.
2. Gravitz L. Liver cancer. Nature 2014;516:S1.
3. Siegel RL, Miller KD, Jemal A. Cancer statistics, 2018. CA Cancer J Clin 2018;68:7–30.
4. Allemani C, Weir HK, Carreira H, Harewood R, Spika D, Wang XS, et al. Global surveillance of cancer survival 1995–2009: analysis of individual data for 25,676,887 patients from 279 population-based registries in 67 countries (CONCORD-2). Lancet 2015;385:977–1010.
5. Allemani C, Matsuda T, Di Carlo V, Harewood R, Matz M, Niksic M, et al. Global surveillance of trends in cancer survival 2000–14 (CONCORD-3): analysis of individual records for 37 513 025 patients diagnosed with one of 18 cancers from 322 population-based registries in 71 countries. Lancet 2018;391:1023–75.
6. Hooks KB, Audoux J, Fazli H, Lesjean S, Ernault T, Dugot-Senant N, et al. New insights into diagnosis and therapeutic options for proliferative hepatoblastoma. Hepatology 2018;68:89–102.
7. Forner A, Reig M, Bruix J. Hepatocellular carcinoma. Lancet 2018;391: 1301–14.
8. Takayasu K, Arii S, Ikai I, Omata M, Okita K, Ichida T, et al. Prospective cohort study of transarterial chemoembolization for unresectable hepatocellular carcinoma in 8510 patients. Gastroenterology 2006; 131:461–9.
9. Lin DC, Mayakonda A, Dinh HQ, Huang P, Lin L, Liu X, et al. Genomic and epigenomic heterogeneity of hepatocellular carcinoma. Cancer Res 2017;77:2255–65.
10. Kopp F, Mendell JT. Functional classification and experimental dissection of long noncoding RNAs. Cell 2018;172:393–407.
11. Fatica A, Bozzoni I. Long non-coding RNAs: new players in cell differentiation and development. Nat Rev Genet 2014;15:7–21.
12. Xing Z, Lin A, Li C, Liang K, Wang S, Liu Y, et al. lncRNA directs cooperative epigenetic regulation downstream of chemokine signals. Cell 2014;159: 1110–25.
13. Peng L, Yuan XQ, Liu ZY, Li WL, Zhang CY, Zhang YQ, et al. High lncRNA H19 expression as prognostic indicator: data mining in female cancers and polling analysis in non-female cancers. Oncotarget 2017;8:1655–67.
14. Peng L, Yuan X, Jiang B, Tang Z, Li GC. LncRNAs: key players and novel insights into cervical cancer. Tumour Biol 2016;37:2779–88.
15. Peng L, Yuan X, Zhang C, Peng J, Zhang Y, Pan X, et al. The emergence of long non-coding RNAs in hepatocellular carcinoma: an update. J Cancer 2018;9:2549–58.
16. Matsumoto A, Pasut A, Matsumoto M, Yamashita R, Fung J, Monteleone E, et al. mTORC1 and muscle regeneration are regulated by the LINC00961-encoded SPAR polypeptide. Nature 2017;541:228–32.
17. Anderson DM, Anderson KM, Chang CL, Makarewich CA, Nelson BR, McAnally JR, et al. A micropeptide encoded by a putative long noncoding RNA regulates muscle performance. Cell 2015;160:595–606.

18. Quinn JJ, Chang HY. Unique features of long non-coding RNA biogenesis and function. Nat Rev Genet 2016;17:47–62.
19. Pott S, Lieb JD. What are super-enhancers? Nat Genet 2015;47:8–12.
20. Hnisz D, Shrinivas K, Young RA, Chakraborty AK, Sharp PA. A phase separation model for transcriptional control. Cell 2017;169:13–23.
21. Hnisz D, Abraham BJ, Lee TI, Lau A, Saint-Andre V, Sigova AA, et al. Super-enhancers in the control of cell identity and disease. Cell 2013;155:934–47.
22. Suzuki HI, Young RA, Sharp PA. Super-enhancer-mediated RNA processing revealed by integrative microRNA network analysis. Cell 2017; 168:1000–14.
23. Hay D, Hughes JR, Babbs C, Davies JOJ, Graham BJ, Hanssen L, et al. Genetic dissection of the alpha-globin super-enhancer *in vivo*. Nat Genet 2016;48:895–903.
24. Jiang YY, Lin DC, Mayakonda A, Hazawa M, Ding LW, Chien WW, et al. Targeting super-enhancer-associated oncogenes in oesophageal squamous cell carcinoma. Gut 2017;66:1358–68.
25. Yuan J, Jiang YY, Mayakonda A, Huang M, Ding LW, Lin H, et al. Super-enhancers promote transcriptional dysregulation in nasopharyngeal carcinoma. Cancer Res 2017;77:6614–26.
26. Pastushenko I, Brisebarre A, Sifrim A, Fioramonti M, Revenco T, Boumahdi S, et al. Identification of the tumour transition states occurring during EMT. Nature 2018;556:463–8.
27. Barriga EH, Franze K, Charras G, Mayor R. Tissue stiffening coordinates morphogenesis by triggering collective cell migration *in vivo*. Nature 2018;554:523–7.
28. Nieto MA, Huang RY, Jackson RA, Thiery JP. EMT: 2016. Cell 2016; 166:21–45.
29. Giannelli G, Koudelkova P, Dituri F, Mikulits W. Role of epithelial to mesenchymal transition in hepatocellular carcinoma. J Hepatol 2016;65:798–808.
30. Reichl P, Haider C, Grubinger M, Mikulits W. TGF-beta in epithelial to mesenchymal transition and metastasis of liver carcinoma. Curr Pharm Des 2012;18:4135–47.
31. Lin DC, Dinh HQ, Xie JJ, Mayakonda A, Silva TC, Jiang YY, et al. Identification of distinct mutational patterns and new driver genes in oesophageal squamous cell carcinomas and adenocarcinomas. Gut 2017;67:1769–79.
32. Lin DC, Hao JJ, Nagata Y, Xu L, Shang L, Meng X, et al. Genomic and molecular characterization of esophageal squamous cell carcinoma. Nat Genet 2014;46:467–73.
33. Whyte WA, Orlando DA, Hnisz D, Abraham BJ, Lin CY, Kagey MH, et al. Master transcription factors and mediator establish super-enhancers at key cell identity genes. Cell 2013;153:307–19.
34. Xie JJ, Jiang YY, Jiang Y, Li CQ, Lim MC, An O, et al. Super-enhancer-driven long non-coding RNA LINC01503, regulated by TP63, is over-expressed and oncogenic in squamous cell carcinoma. Gastroenterology 2018; 154:2137–51.
35. Wheeler TM, Leger AJ, Pandey SK, MacLeod AR, Nakamori M, Cheng SH, et al. Targeting nuclear RNA for *in vivo* correction of myotonic dystrophy. Nature 2012;488:111–5.
36. Soares RJ, Maglieri G, Gutschner T, Diederichs S, Lund AH, Nielsen BS, et al. Evaluation of fluorescence in situ hybridization techniques to study long non-coding RNA expression in cultured cells. Nucleic Acids Res 2018;46:e4.
37. Lennox KA, Behlke MA. Cellular localization of long non-coding RNAs affects silencing by RNAi more than by antisense oligonucleotides. Nucleic Acids Res 2016;44:863–77.
38. Jiang Y, Li Y, Fang S, Jiang B, Qin C, Xie P, et al. The role of MALAT1 correlates with HPV in cervical cancer. Oncol Lett 2014;7:2135–41.
39. Xiao S, Chang RM, Yang MY, Lei X, Liu X, Gao WB, et al. Actin-like 6A predicts poor prognosis of hepatocellular carcinoma and promotes metastasis and epithelial-mesenchymal transition. Hepatology 2016; 63:1256–71.
40. Gao Y, Chen G, Zeng Y, Zeng J, Lin M, Liu X, et al. Invasion and metastasis-related long noncoding RNA expression profiles in hepatocellular carcinoma. Tumour Biol 2015;36:7409–22.
41. Chang RM, Yang H, Fang F, Xu JF, Yang LY. MicroRNA-331–3p promotes proliferation and metastasis of hepatocellular carcinoma by targeting PH domain and leucine-rich repeat protein phosphatase. Hepatology 2014;60:1251–63.
42. Fang JH, Zhou HC, Zhang C, Shang LR, Zhang L, Xu J, et al. A novel vascular pattern promotes metastasis of hepatocellular carcinoma in an epithelial-mesenchymal transition-independent manner. Hepatology 2015;62:452–65.
43. Koutsaki M, Spandidos DA, Zaravinos A. Epithelial-mesenchymal transition-associated miRNAs in ovarian carcinoma, with highlight on the miR-200 family: prognostic value and prospective role in ovarian cancer therapeutics. Cancer Lett 2014;351:173–81.
44. Takai M, Terai Y, Kawaguchi H, Ashihara K, Fujiwara S, Tanaka T, et al. The EMT (epithelial-mesenchymal-transition)-related protein expression indicates the metastatic status and prognosis in patients with ovarian cancer. J Ovarian Res 2014;7:76.
45. Li L, Li W. Epithelial-mesenchymal transition in human cancer: comprehensive reprogramming of metabolism, epigenetics, and differentiation. Pharmacol Ther 2015;150:33–46.
46. Li Z, Dong M, Fan D, Hou P, Li H, Liu L, et al. LncRNA ANCR down-regulation promotes TGF-beta-induced EMT and metastasis in breast cancer. Oncotarget 2017;8:67329–43.
47. Rodriguez-Mateo C, Torres B, Gutierrez G, Pintor-Toro JA. Downregulation of Lnc-Spry1 mediates TGF-beta-induced epithelial-mesenchymal transition by transcriptional and posttranscriptional regulatory mechanisms. Cell Death Differ 2017;24:785–97.
48. Hao Y, Yang X, Zhang D, Luo J, Chen R. Long noncoding RNA LINC01186, regulated by TGF-beta/SMAD3, inhibits migration and invasion through Epithelial-Mesenchymal-Transition in lung cancer. Gene 2017;608:1–12.
49. Kong J, Sun W, Li C, Wan L, Wang S, Wu Y, et al. Long non-coding RNA LINC01133 inhibits epithelial-mesenchymal transition and metastasis in colorectal cancer by interacting with SRSF6. Cancer Lett 2016; 380:476–84.
50. Xu S, Yi XM, Tang CP, Ge JP, Zhang ZY, Zhou WQ. Long non-coding RNA ATB promotes growth and epithelial-mesenchymal transition and predicts poor prognosis in human prostate carcinoma. Oncol Rep 2016;36:10–22.
51. Loven J, Hoke HA, Lin CY, Lau A, Orlando DA, Vakoc CR, et al. Selective inhibition of tumor oncogenes by disruption of super-enhancers. Cell 2013;153:320–34.
52. Dou C, Sun L, Jin X, Han M, Zhang B, Jiang X, et al. Long non-coding RNA CARLo-5 promotes tumor progression in hepatocellular carcinoma via suppressing miR-200b expression. Oncotarget 2017;8:70172–82.
53. Chen L, Yao H, Wang K, Liu X. Long Non-Coding RNA MALAT1 regulates ZEB1 expression by sponging miR-143-3p and promotes hepatocellular carcinoma progression. J Cell Biochem 2017;118:4836–43.
54. Yuan JH, Yang F, Wang F, Ma JZ, Guo YJ, Tao QF, et al. A long noncoding RNA activated by TGF-beta promotes the invasion-metastasis cascade in hepatocellular carcinoma. Cancer Cell 2014;25:666–81.